Diode-Pumped Microchip $Tm:KLu(WO_4)_2$ Laser With More Than 3 W of Output Power

Josep Maria Serres,[1] Xavier Mateos,[1,*] Pavel Loiko,[2] Konstantin Yumashev,[2] Nikolai Kuleshov,[2] Valentin Petrov,[3] Uwe Griebner,[3] Magdalena Aguiló,[1] and Francesc Díaz[1]

[1]Física i Cristal·lografia de Materials i Nanomaterials (FiCMA-FiCNA), Universitat Rovira i Virgili (URV), Campus Sescelades, c/ Marcel·lí Domingo, s/n., Tarragona, Spain E-43007
[2]Center for Optical Materials and Technologies, Belarusian National Technical University, 65/17 Nezavisimosti Ave., Minsk, Belarus 220013
3 Max Born Institute for Nonlinear Optics and Short Pulse Spectroscopy, Max-Born-Str. 2a, Berlin, Germany D-12489
**Corresponding author: xavier.mateos@urv.cat*

Received Month X, XXXX; revised Month X, XXXX; accepted Month X, XXXX; posted Month X, XXXX (Doc. ID XXXXX); published Month X, XXXX

A diode-pumped microchip laser containing a quasi-monolithic plano-plano cavity is realized on the basis of a $Tm:KLu(WO_4)_2$ crystal. The maximum CW output power is 3.2 W (at an absorbed pump power of 6.8 W) and the slope efficiency as high as 50.4%. The laser is operating at 1946 nm in the TEM_{00} mode with a $M^2 < 1.05$. Microchip operation with $Tm:KLu(WO_4)_2$ is in principle due to a special crystal cut along the N_g optical indicatrix axis. This crystal cut possesses positive near-spherical thermal lens that provides the required mode stabilization in the plano-plano cavity. Sensitivity factors of the thermal lens, "generalized" thermo-optic coefficients and constants describing the photoelastic effect are determined for the monolithic $Tm:KLu(WO_4)_2$ crystal. © 2014 Optical Society of America

OCIS Codes: (140.3480) Lasers, diode-pumped, (140.6810) Thermal effects.
http://dx.doi.org/10.1364/OL.99.099999

Monolithic microchip lasers consist of a laser crystal with two flat mirrors attached or directly deposited on the crystal surfaces. Such a device is attractive due to its compact and robust design that is insensitive to misalignment, as well as high efficiency due to absence of losses at the air/crystal interfaces. The mode stabilization in such a plano-plano laser cavity is provided by focusing thermal lens and the gain stabilization mechanism is also known [1]. Thus, laser hosts with negative thermo-optic coefficients (dn/dT) are in general not suitable for microchip laser operation. Sometimes, the microchip laser concept is extended to quasi-monolithic design with at least one plane mirror being in direct contact with the crystal. This option enables for insertion of some additional elements in the cavity, a saturable absorber for Q-switching or a Fabry-Perot etalon for single-frequency operation.

Thulium (Tm) lasers attract attention due to their wavelength-tunable emission in the 1.9-2.0 μm range, a region of interest for medical applications. The first Tm-doped microchip laser was presented by J. Zayhowski using an ***a***-cut $Tm:YVO_4$ crystal [2]. Later, the list of Tm-hosts was extended with $GdVO_4$ [3], YLF [4], YAP [5] and YAG [6], and some optimization was performed with $Tm:YVO_4$ [8]. The highest output power was obtained with Tm:YAP [5] and $Tm:GdVO_4$ [7], reaching 6.2 and 1.4 W, respectively. The highest slope efficiency was achieved with a $Tm:YVO_4$ crystal [2] reaching 44% with respect to the absorbed power (42% with respect to the incident power with 95% absorption in the crystal). Recently, Tm-doped monoclinic double tungstates, well-known class of crystals for efficient diode-pumped lasers [9], were reconsidered for the potential of microchip laser operation [10,11]. The "standard" cut of these crystals propagation direction along the N_p axis of the optical indicatrix is characterized by a negative thermal lens [12]. Other cuts, particularly, along the N_g axis can provide the desired mode stabilization. Orienting a crystal in such a way, a continuous-wave (CW) N_g-cut $Tm:KY(WO_4)_2$ microchip laser delivering 650 mW output power with 44% slope efficiency was realized [10] with comparable slope efficiency as with $Tm:YVO_4$ in [2]. However, it is known that $KLu(WO_4)_2$ (shortly, KLuW) is a more appropriated host for Tm-doping [13], so higher output power and slope efficiency are expected with a Tm:KLuW crystal. In the present paper, we study microchip laser operation of N_g-cut Tm:KLuW crystal achieving the highest slope efficiency (> 50%) of any Tm-doped microchip laser and explain the mechanism of laser mode stabilization from the point of view of thermo-optic effects.

For the present study, monoclinic Tm:KLuW crystal was grown by the Top-Seeded Solution Growth (TSSG) slow-cooling method with the ***b*** crystallographic axis perpendicular to the solution. The content of Tm^{3+}-ions in the solution was 3 at.%, and the actual ion density in the crystal measured by Electron Probe Microanalysis (EPMA) was 2.15×10^{20} at/cm^3. From the as-grown bulk a 2.5 mm thick crystal with an aperture of 3×3 mm^2 was cut. Its short edge was parallel to N_g axis (N_g-cut crystal). The sample of high optical quality was just polished without any coatings deposited. Its four lateral faces were attached to a specially designed water-cooled Cu holder by means of a heat grease compound; the temperature of the holder was fixed at 16°C.

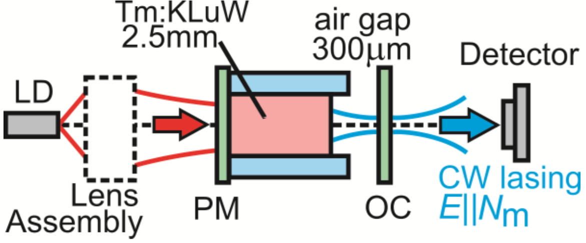

Fig. 1. Setup of the Tm:KLuW microchip laser. Laser diode (LD), pump mirror (PM) and output coupler (OC).

The laser cavity for microchip operation consisted of two plane mirrors. The pump mirror was antireflection (AR) coated for the 770-1050 nm range and high reflection (HR) coated for the 1800-2075 nm range and attached directly to the input face of the crystal. Several output couplers (OCs) with transmission at the laser wavelength (T_{OC}) of 1.5%, 3%, 5% and 9% were employed which were AR-coated (< 2% at 808 nm) on their rear side. All OCs were separated from the output face of the crystal by a 300 μm air gap. Thus, the crystal was pumped in a single-pass configuration.

The pump source was a fiber-coupled laser diode operating at 805-807 nm depending on the current level and delivering a maximum power of 25 W. The fiber had a core diameter of 200 μm and a numerical aperture (NA) of 0.22. To collimate and focus the pump light we used a lens assembly with a focal length of 30 mm providing a 1:1 imaging ratio (meaning a pump spot radius w_p ~ 100 μm). The absorption of the crystal amounted to 62%. A sketch of the compact laser set-up is shown in Fig. 1.

Laser action was achieved for all the output couplers studied. The laser polarization was always parallel to the N_m axis. Figure 2 shows the output power versus the absorbed pump power, P_{abs}, with very similar behavior for all OCs. The maximum output power was 3.16 W for T_{oc} = 5% at P_{abs} = 6.8 W and the minimum threshold was 116 mW for T_{oc} = 1.5%. The laser wavelength was centered typically at 1946 nm (inset in Fig. 2) for all OCs. However, at P_{abs} > 4 W, several wavelengths oscillated simultaneously in the range of 1942-1950 nm. The highest slope efficiency for T_{oc} = 5% amounted to 50.4% fitting the entire range of the absorbed pump power.

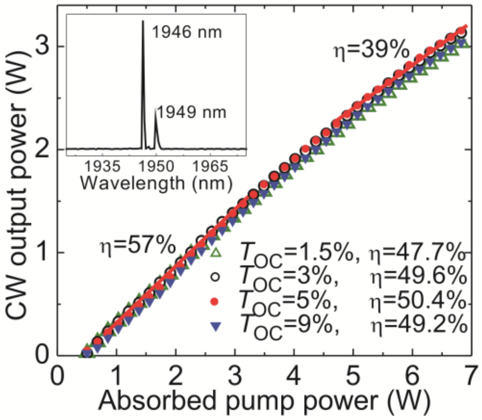

Fig. 2. CW output power of the Tm:KLuW microchip laser as a function of the absorbed pump power; inset represents typical spectrum of output radiation, lines are plotted for T_{OC}=5%.

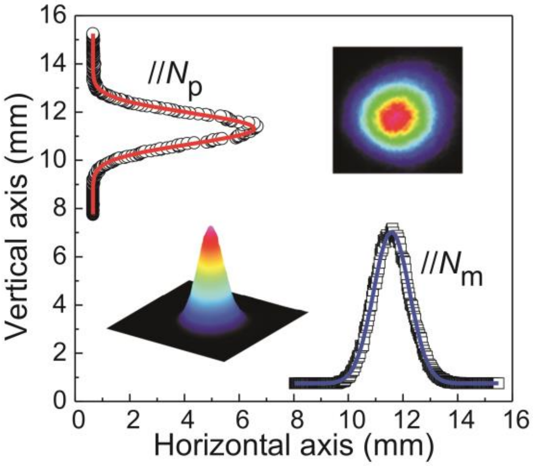

Fig. 3. 2D and 3D beam profiles of the Tm:KLuW microchip laser with Gaussian fits for the sections along the horizontal (// N_m) and vertical (// N_p) axes.

The output beam profile was measured with a FLIR SC7210 thermal imaging camera exhibiting a pixel size of 30 μm. Figure 3 shows the far-field intensity of the microchip laser indicating a TEM_{00} mode characterized by a Gaussian distribution as well as the fits for the horizontal (//N_m) and vertical (//N_p) directions. The measurement was carried out for an intermediate absorbed power (~ 2 W). The M^2 factor was measured to be M^2_x, M^2_y < 1.05.

In order to explain the potential of N_g-cut Tm:KLuW for microchip laser operation, we measured the dioptric optical power of the thermal lens for this crystal, Fig. 4. The experiment was similar to the one presented in [14], the light polarization was $\boldsymbol{E}$ // N_m, and the pump spot radius w_p ~100 μm. The thermal lens in the N_g-cut crystal is positive (that means focusing) for both principal

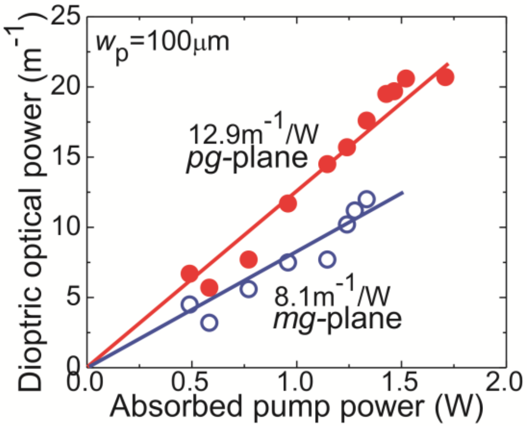

Fig. 4. Dioptric optical power of thermal lens for N_g-cut Tm:KLuW crystal (laser wavelength is 1.95 μm, laser polarization is $\boldsymbol{E} // N_m$, pump spot radius w_p is 100 μm).

meridional planes, namely the *pg*- (M = 12.1 m^{-1}/W) and the *mg*-plane (M = 8.1 m^{-1}/W); M is the sensitivity factor of the thermal lens [15] with respect to the absorbed pump power, $M = \mathrm{d}D/\mathrm{d}P_{abs}$. The experiment was performed for a hemispherical laser cavity (not microchip) in order to get higher sensitivity to the thermal lens influence.

To recalculate the parameters of thermal lens for quasi-"monolithic" laser and to explain beneficial thermo-optic properties of N_g-cut Tm:KLuW crystal, we extract different contributions to the M-factor [15]:

$$M = \frac{\eta_h}{2\pi w_p^2 \kappa}\chi, \quad \chi = \left(\frac{dn}{dT} + P_{PE} + Q_{dist}\right) \qquad (1)$$

Here η_h is the fractional heat loading, w_p is the pump spot radius and κ is the thermal conductivity in the *mp*-plane. The pump beam is considered to be "top-hat" and $\chi = \mathrm{d}n/\mathrm{d}T + P_{PE} + Q_{dist}$ is the "generalized" thermo-optic coefficient [14] including three terms representing the temperature dependence of the refractive index, $\mathrm{d}n/\mathrm{d}T$, the impact of the photoelastic effect, P_{PE}, and the microscopic distortion of crystal end faces (axial strain), Q_{dist}. The corresponding values are listed in Table 1.

In Table 1, χ is calculated directly from the measured M-factors, Eq.(1), $\mathrm{d}n/\mathrm{d}T$ is taken from [16]. Q_{dist} is determined as $(n_m-1)\alpha_g$ where n is the refractive index [9] and α is the thermal expansion coefficient [16] (the expression for Q_{dist} takes into account axial strain related to pure thermal expansion). Thus, the P_{PE} term can be estimated as $P_{PE} = \chi - \mathrm{d}n/\mathrm{d}T - Q_{dist}$. Both, the P_{PE} and χ values have not been reported previously for N_g-cut Tm:KLu(WO$_4$)$_2$. The value of P_{PE} is small and has different signs for *pg*- and *mg*-planes (+1.7 and –1.6 × 10^{-6} K^{-1}). As a result, large thermal expansion that provides positive variation of the optical path length and dominates over negative impact of $\mathrm{d}n/\mathrm{d}T$, as well as a weak photoelastic effect, has major effect on the formation of the positive lens in the N_g-cut crystal.

In our case of a quasi-"monolithic" Tm:KLuW laser, the expression for Q_{dist} will be $(n_m-1/2)\alpha_g$ with the conditions (i) only the pump mirror is in contact with the crystal, and (ii) the bulging occurs on both input and output end faces of the crystal due to a relatively uniform absorption of pump light. Since $\mathrm{d}n/\mathrm{d}T$ and P_{PE} remain unchanged, corrected χ values and M-factors can be evaluated, see Table 1. The latter equal +22.7 m^{-1}/ W and +17.9 m^{-1}/W for *pg*- and *mg*-planes, respectively. Such strong and positive thermal lens is the main factor responsible for mode stabilization in the Tm:KLuW microchip laser. Weak astigmatism of thermal lens ($S = M_{pg} - M_{mg}$ = 4.8 m^{-1}/W, or S/M_{pg} = 20%) results in the near-circular beam profile. At maximum P_{abs} reached in the experiment (6.8 W), focal lengths of the thermal lens are 6.5 mm (*pg*) and 8.2 mm (*mg*-plane).

Table 1 Thermo-Optic Characterization of Diode-Pumped N_g-cut Tm:KLu(WO$_4$)$_2$ Laser Crystal

M-factor, m^{-1}/W	$\mathrm{d}n/\mathrm{d}T$, 10^{-6} K^{-1}	P_{PE}, 10^{-6} K^{-1}	Q_{dist}, 10^{-6} K^{-1}	χ, 10^{-6} K^{-1}
"Laser cavity" configuration				
+12.9 (*pg*)	–5.9	+1.7 (*pg*)	+13.0	+8.8 (*pg*)
+8.1 (*mg*)		–1.6 (*mg*)		+5.5 (*mg*)
Quasi-"monolithic" configuration				
+22.7 (*pg*)	–5.9	+1.7 (*pg*)	+19.6	+15.4 (*pg*)
+17.9 (*mg*)		–1.6 (*mg*)		+12.1 (*mg*)

The principal meridional planes are denoted in brackets.

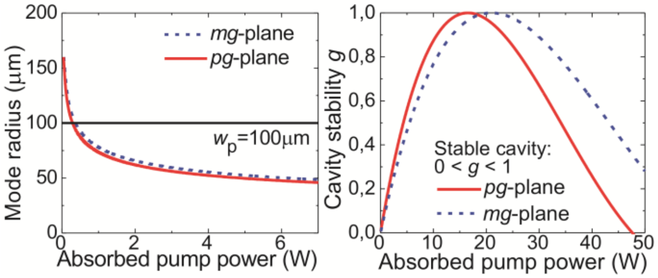

Fig. 5. Mode-matching and cavity stability analysis for a quasi-monolithic Tm:KLu(WO$_4$)$_2$ microchip laser.

We also analyzed the mode-matching and cavity stability of the Tm:KLuW microchip laser from the point of view of thermo-optic effects, see Fig. 5. The selected microchip cavity does not approach the instability limit even at P_{abs} = 6.8 W. The corresponding "critical" point is around 45 W, so further power scaling is possible. From Fig. 5, it becomes obvious that mode-matching is not optimal, as the radius of the laser mode for P_{abs} = 6.8 W is stabilized around 50±5 μm which is lower than in our laser: w_p ~ 100 μm. Therefore our laser operated with substantially reduced efficiency as can be depicted from Fig. 2. The slope for P_{abs} = 2–3 W is 57% and for P_{abs} = 6–7 W only 39%.

The optimization of mode-matching conditions will be the subject of a separate study. We expect that it can result in a slope efficiency approaching 83%, because of the potential quantum yield of 2 due to the cross-relaxation when pumping the Tm-ions around 800 nm.

In conclusion, the microchip laser concept is applied to a Tm:KLuW crystal to demonstrate TEM$_{00}$-mode laser operation with maximum output power higher than 3 W at 1946 nm and demonstrate a slope efficiency as high as 50.4%. The key role of thermally-induced effects for the mode stabilization in the plano-plano cavity is explained. Further improvement will focus on perfect mode-matching between the pump and laser modes to increase the efficiency and output power of this laser as well as on optimization of the doping level and thickness of the active medium.

This work was supported by the Spanish Government under project MAT2011-29255-C02-02, and by the Generalitat de Catalunya under project 2009SGR235. It has been partially funded by the European Commission within the Seventh Framework Programme, under projects Cleanspace and FP7-SPACE-2010-1–GA-263044.

References

1. J.J. Zayhowski and A. Mooradian, Opt. Lett. **14**, 24 (1989).
2. J.J. Zayhowski, J. Harrison, C. Dill, III, and J. Ochoa, Appl. Opt. **34**, 435 (1995)
3. C.P. Wyss, W. Lüthy, H.P. Weber, V.I. Vlasov, Y.D. Zavartsev, P.A. Studenikin, A.I. Zagumennyi, and I.A. Shcherbakov, Appl. Phys. B 67, 545 (1998).
4. T. Yokozawa, J. Izawa, and H. Hara, Opt. Commun. **145**, 98 (1998).
5. J. Sulc, H. Jelinkova, K. Nejezchleb, and V. Skoda, Proc. SPIE **7193**, 71932H (2009).
6. F.F. Heine, and G. Huber, Appl. Opt. **37**, 3268 (1998).
7. C.P. Wyss, W. Luthy, H.P. Weber, V.I. Vlasov, Y.D. Zavartsev, P.A. Studenikin, A.I. Zagumennyui, and I.A. Shcherbakov, IEEE J. Quantum Electron. **34**, 2380 (1998).
8. G. Lescroart, R. Muller, and G. Bourdet, Opt. Commun. **143**, 147 (1997).
9. V. Petrov, M.C. Pujol, X. Mateos, O. Silvestre, S. Rivier, M. Aguiló, R.M. Solé, J. Liu, U. Griebner, and F. Díaz, Laser & Photon. Rev. **1**, 179 (2007).
10. M.S. Gaponenko, P.A. Loiko, N.V. Gusakova, K.V. Yumashev, N.V. Kuleshov, and A.A. Pavlyuk, Appl. Phys. B. **108**, 603 (2012).
11. V.G. Savitski, R.B. Birch, E. Fraczek, A.J. Kemp, P.A. Loiko, K.V. Yumashev, N.V. Kuleshov, and A.A. Pavlyuk, in CLEO/Europe-EQEC 2013, Munich, May, 12-16, 2013, P. CA-10.5.
12. P.A. Loiko, K.V. Yumashev, N.V. Kuleshov, V.G. Savitski, S. Calvez, D. Burns, and A.A. Pavlyuk, Opt. Expr. **17**, 23536 (2009).
13. O. Silvestre, M.C. Pujol, M. Rico, F. Güell, M. Aguiló, and F. Díaz, Appl. Phys. B **87**, 707 (2007).
14. P.A. Loiko, V.G. Savitski, A. Kemp, A.A. Pavlyuk, N.V. Kuleshov, and K.V. Yumashev, Laser Phys. Lett. **11**, 055002 (2014).
15. S. Chenais, F. Druon, S. Forget, F. Balembois, and P. Georges, Progress Quantum Electron. **30**, 89 (2006).
16. P.A. Loiko, K.V. Yumashev, N.V. Kuleshov, G.E. Rachkovskaya, and A.A. Pavlyuk, Opt. Mater. 33, 1688 (2011).

1. J.J. Zayhowski and A. Mooradian, "Single-frequency microchip Nd lasers," Opt. Lett. **14**, 24–26 (1989).
2. J.J. Zayhowski, J. Harrison, C. Dill, III, and J. Ochoa, "Tm:YVO_4 microchip laser," Appl. Opt. **34**, 435–437 (1995)
3. C.P. Wyss, W. Lüthy, H.P. Weber, V.I. Vlasov, Y.D. Zavartsev, P.A. Studenikin, A.I. Zagumennyi, and I.A. Shcherbakov, "Emission properties of a 0.1 mm Tm^{3+}:$GdVO_4$ microchip laser at 1.9 µm," Appl. Phys. B **67**, 545–548 (1998).
4. T. Yokozawa, J. Izawa, and H. Hara, "Mode control of a Tm:YLF microchip laser by a multiple resonator," Opt. Commun. **145**, 98–100 (1998).
5. J. Sulc, H. Jelinkova, K. Nejezchleb, and V. Skoda, "High-efficient room-temperature CW operating Tm:YAP laser with microchip resonator," Proc. SPIE **7193**, 71932H (2009).
6. F.F. Heine, and G. Huber, "Tunable single frequency thulium:YAG microchip laser with external feedback," Appl. Opt. **37**, 3268–3271 (1998).
7. C.P. Wyss, W. Luthy, H.P. Weber, V.I. Vlasov, Y.D. Zavartsev, P.A. Studenikin, A.I. Zagumennyui, and I.A. Shcherbakov, "A diode-pumped 1.4-W Tm^{3+}:$GdVO_4$ microchip laser at 1.9 µm," IEEE J. Quantum Electron. **34**, 2380–2382 (1998).
8. G. Lescroart, R. Muller, and G. Bourdet, "Experimental investigations and theoretical modeling of a Tm:YVO_4 microchip laser," Opt. Commun. **143**, 147–155 (1997).
9. V. Petrov, M.C. Pujol, X. Mateos, O. Silvestre, S. Rivier, M. Aguiló, R.M. Solé, J. Liu, U. Griebner, and F. Díaz, "Growth and properties of $KLu(WO_4)_2$,and novel ytterbium and thulium lasers based on this monoclinic crystalline host," Invited paper in Laser & Photon. Rev. **1**, 179–212 (2007).
10. M.S. Gaponenko, P.A. Loiko, N.V. Gusakova, K.V. Yumashev, N.V. Kuleshov, and A.A. Pavlyuk, "Thermal lensing and microchip laser performance of N_g-cut Tm^{3+}:$KY(WO_4)_2$ crystal," Appl. Phys. B. **108**, 603–607 (2012).
11. V.G. Savitski, R.B. Birch, E. Fraczek, A.J. Kemp, P.A. Loiko, K.V. Yumashev, N.V. Kuleshov, and A.A. Pavlyuk, "The prospects for Yb- and Nd-doped tungstate microchip lasers," in CLEO/Europe-EQEC 2013, Munich, May, 12-16, 2013, P. CA-10.5.
12. P.A. Loiko, K.V. Yumashev, N.V. Kuleshov, V.G. Savitski, S. Calvez, D. Burns, and A.A. Pavlyuk, "Thermal lens study in diode pumped N_g- and N_p-cut Nd:$KGd(WO_4)_2$ laser crystals," Opt. Expr. **17**, 23536–23543 (2009).
13. O. Silvestre, M.C. Pujol, M. Rico, F. Güell, M. Aguiló, and F. Díaz, "Thulium doped monoclinic $KLu(WO_4)_2$ single crystals: growth and spectroscopy," Appl. Phys. B **87**, 707–716 (2007).
14. P.A. Loiko, V.G. Savitski, A. Kemp, A.A. Pavlyuk, N.V. Kuleshov, and K.V. Yumashev, "Anisotropy of the photo-elastic effect in Nd:$KGd(WO_4)_2$ laser crystals," Laser Phys. Lett. **11**, 055002-1–7 (2014).
15. S. Chenais, F. Druon, S. Forget, F. Balembois, and P. Georges, "On thermal effects in solid-state lasers: The case of ytterbium-doped materials," Invited paper in Progress Quantum Electron. **30**, 89–153 (2006).
16. P.A. Loiko, K.V. Yumashev, N.V. Kuleshov, G.E. Rachkovskaya, and A.A. Pavlyuk, "Thermo-optic dispersion formulas for monoclinic double tungstates $KRe(WO_4)_2$ where Re = Gd, Y, Lu, Yb," Opt. Mater. **33**, 1688–1694 (2011).